



Science Arts & Métiers (SAM)

is an open access repository that collects the work of Arts et Métiers Institute of Technology researchers and makes it freely available over the web where possible.

This is an author-deposited version published in: <https://sam.ensam.eu>
Handle ID: <http://hdl.handle.net/10985/23141>



This document is available under CC BY-NC-SA license

To cite this version :

Alisson GOUNON, Soumaya LATOUR, Jean LETORT, Saber EL AREM - Rupture Nucleation on a Periodically Heterogeneous Interface - Geophysical Research Letters - Vol. 49, n°20, p.1 - 2022

Any correspondence concerning this service should be sent to the repository

Administrator : scienceouverte@ensam.eu



Geophysical Research Letters®



RESEARCH LETTER

10.1029/2021GL096816

Key Points:

- We provide experimental observations of rupture nucleation on a periodically heterogeneous interface in mode II
- We observe in some cases an alternation of fast and slow rupture episodes correlated to the position of the heterogeneity
- Despite the rupture velocity changes at small scale, the nucleation is a globally accelerating process at larger scale

Supporting Information:

Supporting Information may be found in the online version of this article.

Correspondence to:

A. Gounon,
alison.gounon@irap.omp.eu

Citation:

Gounon, A., Latour, S., Letort, J., & El Arem, S. (2022). Rupture nucleation on a periodically heterogeneous interface. *Geophysical Research Letters*, 49, e2021GL096816. <https://doi.org/10.1029/2021GL096816>

Received 28 OCT 2021

Accepted 3 OCT 2022

Rupture Nucleation on a Periodically Heterogeneous Interface

A. Gounon¹ , S. Latour¹ , J. Letort¹ , and S. El Arem² 

¹Observatoire Midi Pyrénées, IRAP, CNRS UMR5277, Université Paul Sabatier, Toulouse, France, ²LAMPA, Arts et Métiers Sciences & Technologies, Angers, France

Abstract In this study we explore experimentally the effects of fault heterogeneity on the rupture nucleation. We conducted friction experiments between two polycarbonate plates, with a periodically heterogeneous friction interface. The rupture propagation is monitored with an ultra-fast video camera by taking advantage of the photo-elastic properties of the material used. We show that the nucleation process does not always consists of a monotonic growth of the rupture velocity. Instead, the rupture front advances with an alternation of slow and fast episodes that accelerates until it reaches a point at which fast propagation dominates. This complex nucleation process is compared to the results predicted by previous numerical studies on heterogeneous interfaces. Finally, we test whether it is possible to describe this complex nucleation process as a homogenized nucleation. We also point out a large variability in the rupture process due to the uncontrolled stress heterogeneity that occurs during the loading process.

Plain Language Summary Measurements of earth surface deformation and of small intensity seismicity suggest that some large earthquakes are preceded by slow preparatory processes. Independently, several laboratory experiments, by sliding two blocks of rocks or plastic against one-another, have shown that the slip begins with a so-called initiation phase, during which the slipping area slowly grows until it reaches a size at which it accelerates and produces seismic waves. Whether this kind of initiation process is relevant for earthquakes is debated because these processes have been observed on homogeneous interfaces, very different from natural heterogeneous faults. To address this discrepancy, we mimicked earthquakes in the laboratory by sliding two blocks of plastic against one-another, and observed the slip initiation with an ultra-fast camera. We created an alternation of rough and smooth areas at the interface by roughening them with two different kinds of sandpaper. We observed a complex initiation process that consists of an accelerating alternation of slow and rapid episodes that enlarge the slipping area until the final large and fast rupture is triggered. These observations suggest that, on real faults, slow slip and seismic precursors could both be related as parts of a global complex initiation process.

1. Introduction

Understanding how earthquakes initiate on active faults and whether this initiation could be detected is an issue of foremost importance in seismology. However, because the physical process of co-seismic rupture corresponds to the development of an instability, its physics is highly non-linear, and involves many scale-dependent processes. This leads to fundamental challenges in studying rupture initiation and propagation whether theoretically, numerically, or experimentally.

In several laboratory friction experiments, a so-called nucleation or initiation phase, also referred to as “preparatory process,” has been identified prior to fast rupture propagation (Gvirtzman & Fineberg, 2021; Latour et al., 2013; McLaskey, 2019; Ohnaka & Shen, 1999; Passelègue et al., 2017; Yamashita et al., 2021). These studies show a continuously growing slipping area as a nucleation process on homogeneous interfaces, while complexity arises in the preparatory process on randomly heterogeneous interfaces. Theoretically, a critical nucleation size that depends on normal stress, material elasticity, and friction parameters is predicted on homogeneous faults (Ionescu & Campillo, 1999; Rice et al., 2001; Rubin & Ampuero, 2005). A critical length has also been identified in some experiments with homogeneous interfaces (Latour et al., 2013; Ohnaka & Shen, 1999). The concepts of effective friction parameters and effective critical nucleation length have been further introduced to extend the understanding of the nucleation process to heterogeneous interfaces, periodical (Campillo et al., 2001; Cattania & Segall, 2021; Dascalu et al., 2000; Dublanchet, 2018; Favreau et al., 1999; Latour et al., 2011; Schär et al., 2021; Yabe & Ide, 2018) or random (Albertini et al., 2021; Dublanchet et al., 2013; Lavalée, 2008; Lebihain et al., 2021; Schär et al., 2021).

© 2022. The Authors.

This is an open access article under the terms of the [Creative Commons Attribution License](https://creativecommons.org/licenses/by/4.0/), which permits use, distribution and reproduction in any medium, provided the original work is properly cited.

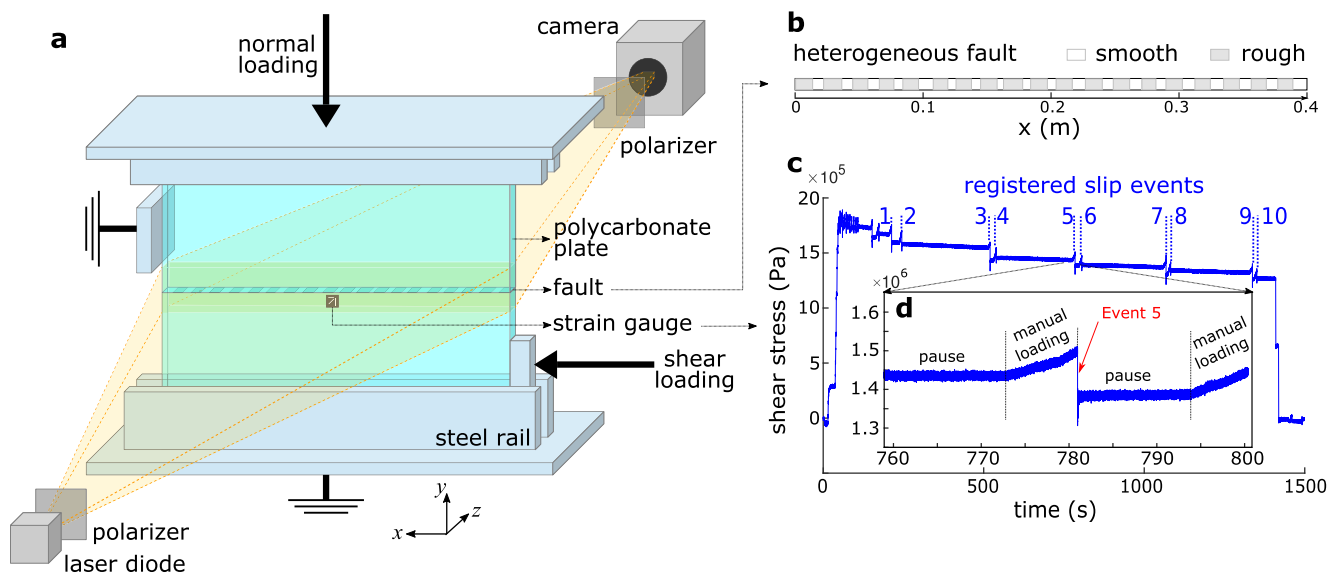


Figure 1. (a) Principle of the experimental set-up (see Text and Supporting Information S1 for details). (b) Sketch of the upper side of the heterogeneous interface. (c) Shear stress at the strain gauge location during an experiment (Experiment 3—heterogeneous), and (d) a zoom on event 5.

However, it is not straightforward to connect those fundamental results to geophysical observations of natural seismicogenic faults. Several observations suggest that a form of preparatory process occurs prior some earthquakes. For example, occurrence of foreshock sequences, during which repeating events and migration of seismicity are observed, could be interpreted as the results of a large and slowly growing nucleation zone affected by slow slip, in which small asperities break, sometimes repeatedly (Bouchon et al., 2011; Nadeau & McEvilly, 1999; Uchida et al., 2003, 2016). Moreover, geodetic observations showed that slow slip occurred before large earthquakes, but it is difficult to quantify how much of this deformation is accounted for by the foreshock sequence and its post-seismic relaxation, and how much of it could be due to silent slow slip (Bouchon et al., 2013; Kato et al., 2012; Ruiz et al., 2014). At least some foreshock sequences might be due to a large scale nucleation process and related to fault heterogeneity. But how exactly the slip develops during initiation on heterogeneous faults and how it partitions between slow silent slip and fast seismic foreshocks is still largely unclear, despite some insights provided by 2D and 3D numerical simulations (Dascalu et al., 2000; Dublanchet et al., 2013; Favreau et al., 1999; Ionescu & Campillo, 1999; Latour et al., 2011; Sudhir & Lapusta, 2020; Yabe & Ide, 2018), as well as by friction experiments using rocks (Dresen et al., 2020; McLaskey, 2019; Passelègue et al., 2017; Wu & McLaskey, 2019; Yamashita et al., 2021).

In this study we aim to produce experimentally a direct observation of the rupture nucleation on a heterogeneous interface with a periodic friction heterogeneity. We produce slip events on an almost 1D interface and observe the rupture nucleation and propagation by photo-elasticity. We introduce friction heterogeneity by varying spatially the roughness of the interface. We present here some interesting observations that show that a large scale globally accelerating nucleation process can develop on a heterogeneous fault, while the details of the rupture propagation are controlled at smaller scale by the friction heterogeneity. We discuss their relevance with respect to recent theoretical developments and to what is known about earthquake preparatory processes.

2. Methods

We produce laboratory earthquakes between two polycarbonate plates ($400 \times 200 \times 9$ mm) set inside a bi-axial loading apparatus controlled by two manual pumps (see Figure 1 and Figure S1 in Supporting Information S1). The plates are maintained by horizontal rails and are in contact through their thin and long sides (400×9 mm). A uni-axial stress around 3 MPa is first imposed in the direction normal to the fault. Then, the lower plate is pushed in the direction parallel to the fault while the upper plate is blocked by a metallic part, until slip occurs between the plates. A stick-slip behavior then takes place, in which each slip event is considered as a laboratory earthquake (Figures 1c and 1d).

One strain gauge rosette placed near the fault (1 cm) at middle length (200 mm) measures the local strain tensor at 4,800 Hz during the experiment. This allows to retrieve the local stresses and to extract the normal and shear stress values just before and after each event, and thus the stress drop. As this strain gauge is the only stress measurement available in our experimental setup, these values will be used as a proxy for the shear stress, residual stress, and stress drop of the whole event (see Figure S5 in Supporting Information S1).

The use of polycarbonate, which is a photo-elastic material, allows to follow the rupture propagation along the fault over time by photo-elasticity, as proposed in several publications (Latour et al., 2013; Nielsen et al., 2010; Schubnel et al., 2011; Xia et al., 2004). The optical setup (see Text S2 in Supporting Information S1) allows to get movies at 170,000 fps of a field of 1280×32 pixels that encompasses almost the whole fault. In these movies, the rupture front propagation can be followed because it is surrounded by stress field variations (stress concentration followed by stress drop) that create light intensity variations. We plot the light intensity variation for a line of pixels parallel to the fault at each time step, creating videograms (Figures 2a, 2c and 2e). The rupture front position at successive time steps is extracted by manually picking its position on the videograms (Figure S7 in Supporting Information S1). This finally allows to obtain the rupture propagation history of the events (Figures 2b, 2d, 2f, and Figures S8–S10 in Supporting Information S1) and to estimate a nucleation length by measuring the length of the rupture when it reaches its final constant velocity (see Text S4 in Supporting Information S1).

Three types of interfaces were studied: (a) smooth (homogeneous), (b) rough (homogeneous), and (c) heterogeneous interfaces. The smooth interface was prepared by manually sanding both sides of the interface with A800 (smooth) sandpaper. For the rough interface we used A800 sandpaper on the lower side, and A400 (rougher) sandpaper on the upper side. The heterogeneous interface (Figure 1b) is composed on the upper side by an alternation of rough and smooth parts approximately 1 cm long (with irregularities due to the manual sanding process). The lower side is sanded homogeneously with the finest A800 sandpaper.

For each kind of interface, several runs of the experiment have been realized during which 10 slip events are registered by applying the procedure described in Text S1 in Supporting Information S1. This leads to a total of 40 registered events for the heterogeneous interface and 20 for the smooth and rough interfaces.

3. Results

The videograms of three events chosen for their representativeness are presented in Figures 2a, 2c and 2e. For the three events, the rupture initiates around the position $x = 35 \pm 3$ cm on the fault. This is the case for all the events of all the experiments, and is most probably a result of the loading geometry, as will be shown later in Section 5.

3.1. Smooth Interface

The nucleation of the representative event on the smooth interface (Figures 2a and 2b) consists of a transition from very low to high rupture velocity over a distance of 4 cm. The rupture is unilateral, meaning that it propagates only toward one direction (from right to left of the figure). The rupture velocity growth is not monotonic and one decelerating episode can be seen (see Figure 2b). Such a behavior is also observed in the majority (12) of the smooth events. However, a monotonic rupture velocity growth is also observed for eight events (Figure 2g). The rupture front position for all the events on smooth interface is shown in Figures S8, S11, and S12 in Supporting Information S1, to demonstrate the variability of rupture behaviors. The mean nucleation length is $\langle L_S \rangle = 3.8$ cm, with standard deviation $\sigma_{L_S} = 3.0$ cm (see Figure 3a).

3.2. Rough Interface

The nucleation of the representative event on the rough interface (Figures 2c and 2d) consists of a continuous and monotonic transition from low to high rupture velocity. This nucleation process occurs on an area approximately 14 cm wide, and is unilateral. When considering the 20 events measured on the rough interface (see Figures S9, S13, and S14 in Supporting Information S1), one can see that the nucleation process is monotonic for their majority (17/20). The mean nucleation length is $\langle L_R \rangle = 11.7$ cm, with standard deviation $\sigma_{L_R} = 2.2$ cm (see Figure 3a).

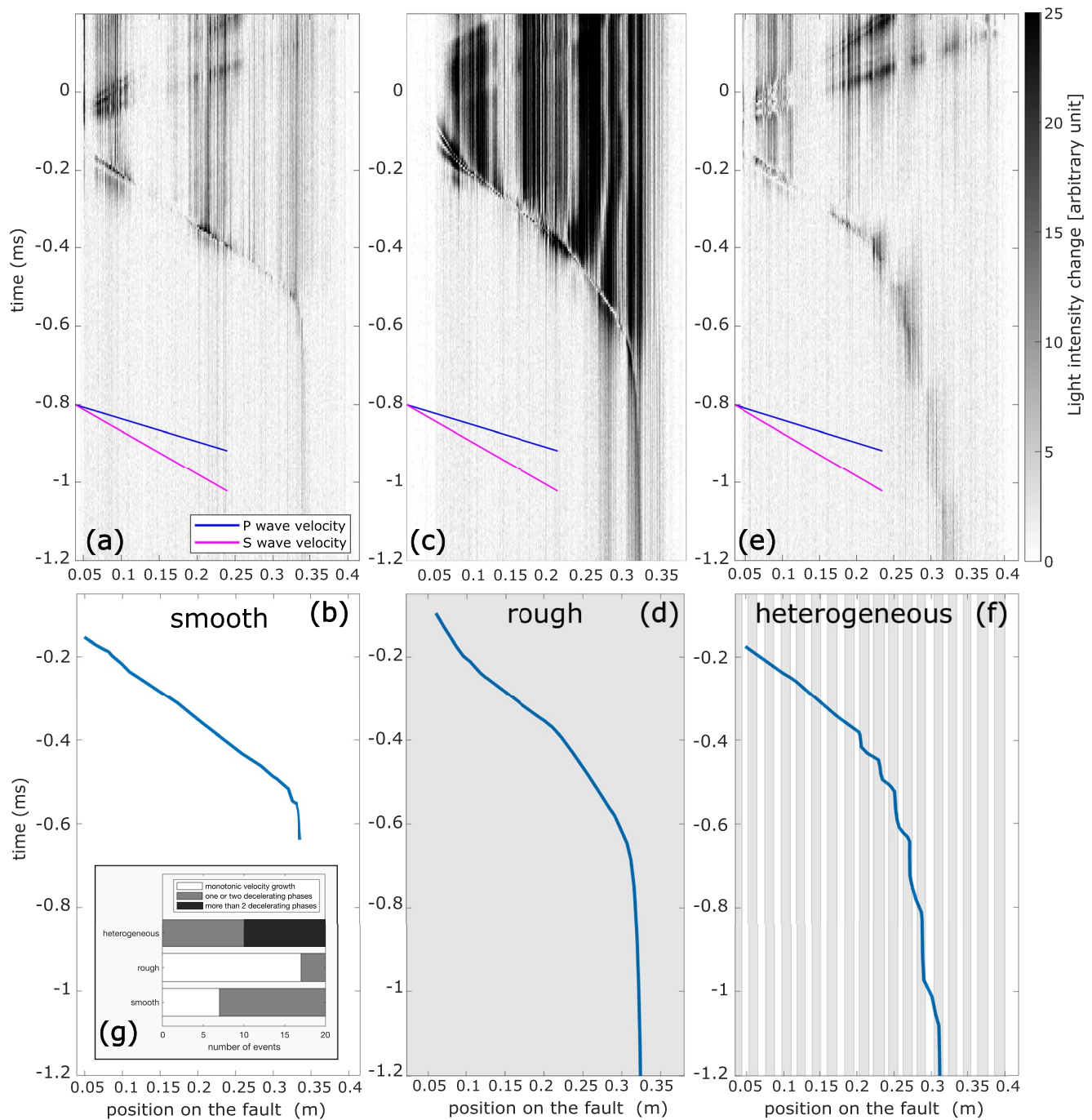


Figure 2. Videograms of typical events on the three types of interfaces and the retrieved space-time evolution of the rupture front for the same events. (a, b): An event with smooth homogeneous interface (event 5 of Experiment 2). The nucleation part starts around $t = -0.6$ ms and $x = 0.35$ m and finish at $t = -0.5$ ms, time at which the “rapid propagation” part begins. (c, d): An event with the rough homogeneous interface (event 9 of Experiment 1). The nucleation begins around $x = 0.32$ m at $t = -1.77$ ms and let the propagation parts starts around $x = 0.2$ m at $t = -0.39$ ms. (e, f): An event with heterogeneous interface (event 4 of Experiment 3). A complex nucleation occurs between $t = -1.7$ and $t = -0.4$ ms, beginning at $x = 0.32$ m and finishing at $x = 0.22$ m where a fast propagation at constant velocity begins. Inset (g) shows the distribution of the three “classes” of nucleation observed for each type of interface.

3.3. Heterogeneous Interface

A rupture event on the heterogeneous interface is described in Figures 2e and 2f, as an example of the specific behavior produced by heterogeneities. A complex phase that we will identify as a complex nucleation occurs between $t = -1.7$ and $t = -0.4$ ms, on the right side of the fault (0.35–0.22 m). During this nucleation process,

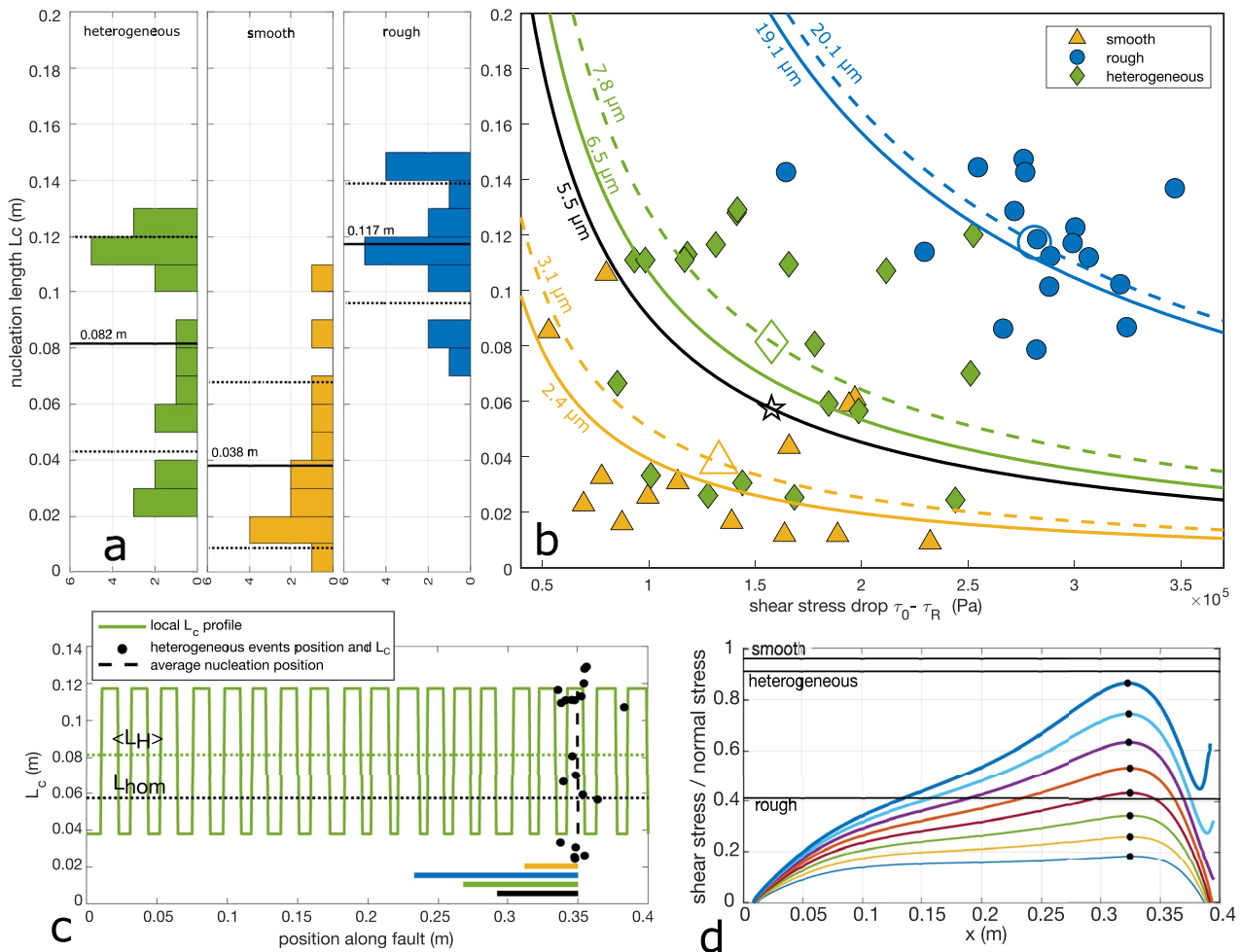


Figure 3. (a) Distribution of the nucleation lengths for the three types of interfaces, and their mean value (continuous line) and standard deviation (dashed lines). (b) Nucleation length versus stress drop for all the events. The large unfilled symbols are placed at the average stress drop and average nucleation length for each type of interface. The continuous colored curves correspond to Equation 1 with best fitting value of D_c for each interface. The dashed colored lines are obtained with Equation 1 and the average stress drop and nucleation length. The continuous black line is obtained with the theoretical homogenized nucleation length and the average stress drop for heterogeneous interface. The curves are labeled with the corresponding values of D_c . (c) Profile of L_c on the heterogeneous fault, of the theoretical homogenized nucleation length L_{hom} and of the average value of L_c on the heterogeneous fault $\langle L_H \rangle$. Bars of lengths $\langle L_S \rangle$, $\langle L_R \rangle$, $\langle L_H \rangle$, and $\langle L_{hom} \rangle$ have been placed for comparison with the heterogeneity size. (d) Successive profiles of the ratio shear stress/normal stress during the numerical simulation of the loading process.

the rupture velocity shows an alternation of slow and fast stages. The duration of the slow stages becomes shorter and shorter along the process until the “fast propagation” phase begins at $t = -0.4$ ms. The rupture front positions for the 40 slip events are plotted in Figures S10, S15, and S16 in Supporting Information S1. Overall, the main observation is a high variability of rupture characteristics (velocity, existence, and duration of the nucleation). The variability is higher between events from different experiments, suggesting that at least some part of the observed behavior is determined by initial conditions that are created when the plates are brought into contact and subjected to normal stress. In the following, we decided to focus on the results of Experiments 3 and 4 with heterogeneous interfaces. In these experiments, complex but reproducible nucleation phases due to the friction heterogeneity are observed, and the nucleation stage can generally be identified: for these 20 events, the measured nucleation length range from 2.5 to 12.9 cm, with a mean value $\langle L_H \rangle = 8.2$ cm and a standard deviation of $\sigma_{L_H} = 3.8$ cm (see Figure 3a).

Interestingly, the rupture velocity variations observed during the complex nucleation phases occur at the same positions for all events. The positions of these transitions are correlated with the locations of smooth and rough parts of the fault (white and gray patches on Figure 2f, respectively). More precisely, each time a rupture enters a

rough portion of the fault, it first decelerates and then propagates at slow velocity for a few millimeters. It finally re-accelerates and then crosses the rest of the rough part and the following smooth part at high velocity, until the next rough portion (or the beginning of the fast propagation phase).

Finally, these complex nucleation phases can be described as a globally accelerating process at large scale, despite the velocity variations at small scale. Indeed, as can be seen in Figure 2f, the maximum rupture velocity reached in each smooth part of the fault grows from the beginning to the end of the nucleation process. Similarly, the delay imposed by each of the very slow stages decreases at each step.

4. Discussion

In this part, we will discuss and explain how we interpret several aspects of these observations.

First, to understand why there is a privileged nucleation position, we used the software Abaqus to simulate the stress state resulting from the loading process (see Text S5 in Supporting Information S1). This stress profile, represented by the ratio of shear stress to normal stress (Figure 3d), is peaked at the typical location where we observe the beginning of nucleations. The length scale of this variation is of the order of the fault length, $\lambda_{setup} \simeq 40$ cm. It is most probable that a random heterogeneity of stress at a smaller length scale and amplitude disturbs this theoretical profile: this type of effect was measured in the experimental setups of Yamashita et al. (2021), Guérin-Marthe et al. (2019), and Bayart et al. (2016, 2018). It arises from the contacting process, that cannot be simultaneous and equally distributed along the interface. If such a random heterogeneity exists, its realization changes each time the fault is unloaded and reloaded (thus between different experiments) and should be slightly but not significantly changed between different successive slip events as was shown in the cited studies. This supposed heterogeneity of stress would be a good candidate to explain part of the variability observed between experiments and between events.

Second, if we consider the whole range of preparatory processes observed in this study, we can classify them in two types of behavior: (a) the “classical” nucleation described for example, in Latour et al. (2013) and Ohnaka and Shen (1999), during which the rupture velocity grows in a monotonic and continuous way and (b) “complex” nucleation in which the rupture grows by successive accelerating and decelerating phases. Among these “complex” nucleation events, we can distinguish between events with only one or two decelerating phases, and those with more than two (see Figure 2g). These diverse types of preparatory processes had already been described for randomly heterogeneous interfaces (Xu et al., 2018; Yamashita et al., 2018, 2021): more complex nucleations arose on more heterogeneous interfaces. Thus, the complexity of preparatory process seems to be characteristic of heterogeneous interfaces. In our experiment, moreover, the periodical friction heterogeneity clearly is the source of the complexity observed at the same scale in the nucleation process. However, some complexity is also present for the supposedly homogeneous interfaces, showing that another source of heterogeneity is also present, probably resulting from the contacting and loading process.

We plot L_C versus the stress drop ($\tau_0 - \tau_R$) measured at mid-fault in Figure 3b. Although dispersed, the data for the three types of interfaces are partitioned into three overlapping yet distinguishable groups. We can thus assume that the mean values of $\tau_0 - \tau_R$ and L_C (large empty symbols in Figure 3b) are representative of a characteristic behavior for each type of interface.

It has been shown theoretically that on homogeneous linear slip-weakening interfaces the critical nucleation length L_C is related to the weakening rate W of the friction law by (Campillo & Ionescu, 1997; Dascalu et al., 2000; Uenishi & Rice, 2003):

$$L_C = 1.158 \frac{\mu^*}{W} = 1.158 \frac{\mu^* D_C}{\tau_P - \tau_R} \quad (1)$$

where $W = (\tau_P - \tau_R)/D_C$, with τ_P the peak shear stress, τ_R the residual shear stress, and D_C the characteristic slip-weakening distance. $\mu^* = \mu/(1 - \nu)$ for mode II ruptures, μ being the shear modulus, and ν the Poisson ratio. If we assume that the stress drop measured at $x = 0.2$ m is representative of the strength drop at the nucleation site, we can use Equation 1 to estimate characteristic values for D_C , either by using the mean values of L_C and $\tau_0 - \tau_r$ (dashed curves in Figure 3b) or by a least square fit (continuous curves).

First, one can remark that the data are not well described by this homogeneous model, even for the homogeneous interfaces. This may be explained by the fact that we approximate the strength drop by the stress drop measured at mid-fault. But it also suggests that there is a source of variability not directly related to the interface properties. Moreover, the theoretical nucleation length of Equation 1 may not correspond exactly to the measured experimental length (see Supporting Information S1). The estimated D_C thus may not be accurate. Nevertheless, the relative values can be compared for the different types of interfaces. It is interesting to see that, as expected from Ohnaka and Shen (1999), the characteristic D_C for the rough interface is larger than the characteristic D_C for the smooth interface. More interestingly, we obtain a characteristic value of D_C for the heterogeneous interface that lays in between the values for the smooth and the rough one. This D_C can be seen as an effective value that homogenizes the effect of the friction heterogeneity on the critical nucleation length.

Alternatively, one can interpret the measured nucleation length as a critical Griffith's length (Andrews, 1976) and estimate a fracture energy characteristic to each interface (see Figure S19 in Supporting Information S1). This process is subject to the same limitations and uncertainties as the previous estimations of D_C . It gives values in the range of 0.07–0.18 J.m⁻² for the “smooth” interface, 0.3–0.59 J.m⁻² for the rough interface, and 2.00–2.58 J.m⁻² for the heterogeneous interface, which are roughly in agreement with other experimental estimations (e.g., 1.1 J.m⁻² for optically flat PMMA in Svetlizky and Fineberg (2014)).

Introducing heterogeneity in the theoretical models of nucleation drastically complicates them, because the slip development at one point of the fault directly depends on the ability of neighboring regions to slip or not. To simplify the problem, the heterogeneity is generally introduced in theoretical studies through one physical parameter only: initial stress (Cattania & Segall, 2021); peak stress τ_P of the friction law with W constant (Schär et al., 2021) or with D_C constant (Campillo et al., 2001); varying weakening rate W with τ_P constant (Lebihain et al., 2021). In contrast, in experimental setups, and also on actual seismogenic faults, the heterogeneity arises both from the friction and stress distribution, and at several length scales. In our study, the friction heterogeneity is imposed at a precise length scale of 2 cm (see Figure 3c). However, on one hand the three friction parameters may vary, and on another hand, an uncontrolled heterogeneity of the stress and/or of the contact is also present. It is thus challenging to compare directly these results with the available theoretical studies. Nevertheless, recent studies (Albertini et al., 2021; Lebihain et al., 2021; Schär et al., 2021) have shown a number of theoretical results that provide a framework to discuss our observations.

Schär et al. (2021) demonstrate three typical behaviors when the heterogeneity is a periodic variation of τ_P of wavelength λ : *classical nucleation* when $\lambda \gg L_C$, *critical coalescence* when $\lambda \simeq L_C$, and *sub-critical coalescence* when $\lambda \ll L_C$. In this subcritical coalescence regime, the rupture length grows by the successive coalescence of asperities in an accelerating process that strongly resembles the complex nucleation described on our heterogeneous interface. Here the wavelength of the heterogeneity is $\lambda = 2$ cm which we can compare either to $\langle L_S \rangle = 3.8$ cm, in which case we should rather be in a critical coalescence regime, or to $\langle L_R \rangle = 11.7$ cm which should correspond to sub-critical coalescence. This is coherent with the fact that we both observe events with up to seven acceleration stages, and events with only one or two acceleration stages. However, it is not possible to resolve with certainty with our setup whether the asperities are slowly slipping together before joining in a true *coalescence* process, or if they begin to slip sequentially one after the other.

Lebihain et al. (2021) show that on interfaces with homogeneous τ_P and heterogeneous W , the profile of W can be used to compute a profile of *local effective* nucleation length and to define a *homogenized* nucleation length L_{hom} , obtained from the average value W_m of the distribution through Equation 1. By using the mean values of L_C on the smooth and rough interface, $\langle L_R \rangle = 11.7$ cm and $\langle L_S \rangle = 3.8$ cm we find $W_R = 14.0$ GPa/m and $W_S = 43.3$ GPa/m, leading to $W_m = 28.6$ GPa/m and $L_{\text{hom}} = 5.8$ cm (see Figures 3b and 3c). Lebihain et al. (2021) identify three regimes (local, extremal, and homogenized) depending on the compared values of the asperities size ξ , the minimum value of the local L_C profile and the homogenized nucleation length L_{hom} . Here we have $\xi = 1$ cm, $L_{\text{min}} = L_{\text{smooth}} = 3.8$ cm, and $L_{\text{hom}} = 5.8$ cm, thus $\xi < L_{\text{min}}$ and $\xi < L_{\text{hom}}$. If we were in the case $\xi \ll L_{\text{min}}$ and $\xi \ll L_{\text{hom}}$ we should observe a homogenized regime and measure nucleation lengths $\simeq L_{\text{hom}} = 5.8$ cm on the heterogeneous interface. The mean value measured is $\langle L_H \rangle = 8.2$ cm, 42% larger than L_{hom} . However, this mean value reflects a very dispersed distribution, thus this deviation is not surprising. Indeed in Figure 3b, the theoretical homogenized regime (black curve) is not far from the best fit for the heterogeneous data (green continuous). Moreover, we actually are at the limit of the homogenized regime, because here $\xi < L_{\text{min}}$ and $\xi < L_{\text{hom}}$. This explains first that the effect of the asperities can be distinguished, and second, that we can

have considerable variations of the measured L_C compared to L_{hom} , that can result from the actual value of the *local effective nucleation length* at the location of the peak stress distribution. We are thus probably at the limit between homogenizable and extremal regimes.

Our observations can also be related to the numerical results of Yabe and Ide (2018) obtained on periodically 1D heterogeneous friction interface. They describe a “dynamic nucleation phase” that can occur with favorable friction conditions, in which slow slip and seismic ruptures of asperities work together in order to prepare the total rupture of the fault. Similarly, Cattania and Segall (2021) introduced heterogeneity in numerical models via interface roughness, and show that the nucleation process consists of “episodic asperity failure, mediated by aseismic slip.” These numerical models fall in range with our observations, where the successive fast ruptures are related to each other by slow propagation phases.

5. Conclusion

In this paper we provide a direct experimental observation of the rupture nucleation on a periodically heterogeneous interface in a 2D in-plane geometry. Despite a high variability between different slip events, we gather several observations of a complex nucleation process in which the variation of interface roughness plays an important role. The rupture propagation begins with an alternation of slow and fast episodes that can be interpreted as a nucleation process, and then reach a last fast phase that breaks the whole interface length (propagation phase). The nucleation process, composed of slow and fast phases, depicts a globally accelerating phenomenon, and can be viewed on the larger scale as a growing nucleation zone in which the slip is partly seismic and partly aseismic. The final length and duration of the large scale nucleation process is thus a result of the rupture propagation dynamics at the smaller scale, and could be seen as an effective nucleation process that homogenizes the small scale friction heterogeneity, as was proposed in previous theoretical studies (Campillo et al., 2001; Dublanchet, 2018; Favreau et al., 2002; Latour et al., 2011; Lebihain et al., 2021; Schär et al., 2021). We tested the theoretical process of homogenization of the friction parameters, in the limits allowed by the available measurements and the restrictive hypotheses of most theoretical studies, and found a general agreement. Although it is not straightforward to generalize these observations to the case of 2D heterogeneous faults, they provide some insights in the current epistemological debate for the conceptualization of earthquake nucleation, and point to models in which slow and fast slip can co-exist during the nucleation process, and in which random heterogeneity of the faults plays an important role.

Data Availability Statement

The data set obtained from our experiments can be found on Zenodo with the <https://doi.org/10.5281/zenodo.6373404> under the name “Experimental observations about rupture nucleation process.” The data are accessible without access conditions.

Acknowledgments

The experimental apparatus was conceived and built with the technical support of the GIS service of OMP (René Dorignac, Pierre Nougé, Marcel Belot, Yoan Micheau, and Driss Kouach). We acknowledge the technical support of Sébastien Benahmed, Michel Dupieu, and Hélène Pauchet, and the participation of François Larrouturnou in developing analysis codes. We are grateful to Alexandre Schubnel, Stefan Nielsen, François Passelègue, and Mathias Lebihain for insightful discussions and/or sharing their experience on experimental setups and to the two anonymous reviewers. This work was financially supported by OMP and IRAP.

References

- Albertini, G., Karrer, S., Grigoriu, M. D., & Kammer, D. S. (2021). Stochastic properties of static friction. *Journal of the Mechanics and Physics of Solids*, 147, 104242. <https://doi.org/10.1016/j.jmps.2020.104242>
- Andrews, D. (1976). Rupture velocity of plane strain shear cracks. *Journal of Geophysical Research*, 81(32), 5679–5687. <https://doi.org/10.1029/jb081i032p05679>
- Bayart, E., Svetlizky, I., & Fineberg, J. (2016). Fracture mechanics determine the lengths of interface ruptures that mediate frictional motion. *Nature Physics*, 12(2), 166–170. <https://doi.org/10.1038/nphys3539>
- Bayart, E., Svetlizky, I., & Fineberg, J. (2018). Rupture dynamics of heterogeneous frictional interfaces. *Journal of Geophysical Research: Solid Earth*, 123(5), 3828–3848. <https://doi.org/10.1002/2018JB015509>
- Bouchon, M., Durand, V., Marsan, D., Karabulut, H., & Schmittbuhl, J. (2013). The long precursory phase of most large interplate earthquakes. *Nature Geoscience*, 6(4), 299–302. <https://doi.org/10.1038/ngeo1770>
- Bouchon, M., Karabulut, H., Aktar, M., Özalaybey, S., Schmittbuhl, J., & Bouin, M.-P. (2011). Extended nucleation of the 1999 M_w 7.6 Izmit earthquake. *Science*, 331(6019), 877–880. <https://doi.org/10.1126/science.1197341>
- Campillo, M., Favreau, P., Ionescu, I. R., & Voisin, C. (2001). On the effective friction law of a heterogeneous fault. *Journal of Geophysical Research*, 106(B8), 16307–16322. <https://doi.org/10.1029/2000JB900467>
- Campillo, M., & Ionescu, I. R. (1997). Initiation of antiplane shear instability under slip dependent friction. *Journal of Geophysical Research*, 102(B9), 20363–20371. <https://doi.org/10.1029/97JB01508>
- Cattania, C., & Segall, P. (2021). Precursory slow slip and foreshocks on rough faults. *Journal of Geophysical Research: Solid Earth*, 126(4), e2020JB020430. <https://doi.org/10.1029/2020jb020430>

- Dascalu, C., Ionescu, I. R., & Campillo, M. (2000). Fault finiteness and initiation of dynamic shear instability. *Earth and Planetary Science Letters*, 177(3–4), 163–176. [https://doi.org/10.1016/S0012-821X\(00\)00055-8](https://doi.org/10.1016/S0012-821X(00)00055-8)
- Dresen, G., Kwiatek, G., Goebel, T., & Ben-Zion, Y. (2020). Seismic and aseismic preparatory processes before large stick–slip failure. *Pure and Applied Geophysics*, 177(12), 5741–5760. <https://doi.org/10.1007/s00024-020-02605-x>
- Dublanche, P. (2018). The dynamics of earthquake precursors controlled by effective friction. *Geophysical Journal International*, 212(2), 853–871. <https://doi.org/10.1093/gji/ggx438>
- Dublanche, P., Bernard, P., & Favreau, P. (2013). Interactions and triggering in a 3-D rate-and-state asperity model. *Journal of Geophysical Research: Solid Earth*, 118(5), 2225–2245. <https://doi.org/10.1002/jgrb.50187>
- Favreau, P., Campillo, M., & Ionescu, I. R. (1999). Initiation of in-plane shear instability under slip-dependent friction. *Bulletin of the Seismological Society of America*, 89(5), 1280–1295. <https://doi.org/10.1785/BSSA0890051280>
- Favreau, P., Campillo, M., & Ionescu, I. R. (2002). Initiation of shear instability in three-dimensional elastodynamics. *Journal of Geophysical Research*, 107(B7), ESE 4-1–ESE 4-18. <https://doi.org/10.1029/2001JB000448>
- Guérin-Marthe, S., Nielsen, S., Bird, R., Giani, S., & Di Toro, G. (2019). Earthquake nucleation size: Evidence of loading rate dependence in laboratory faults. *Journal of Geophysical Research: Solid Earth*, 124(1), 689–708. <https://doi.org/10.1029/2018jb016803>
- Gvirtsman, S., & Fineberg, J. (2021). Nucleation fronts ignite the interface rupture that initiates frictional motion. *Nature Physics*, 17(9), 1037–1042. <https://doi.org/10.1038/s41567-021-01299-9>
- Ionescu, I. R., & Campillo, M. (1999). Influence of the shape of the friction law and fault finiteness on the duration of initiation. *Journal of Geophysical Research*, 104(B2), 3013–3024. <https://doi.org/10.1029/1998JB900090>
- Kato, A., Obara, K., Igarashi, T., Tsuruoka, H., Nakagawa, S., & Hirata, N. (2012). Propagation of slow slip leading up to the 2011 M_w 9.0 Tohoku-Oki Earthquake. *Science*, 335(6069), 705–708. <https://doi.org/10.1126/science.1215141>
- Latour, S., Campillo, M., Voisin, C., Ionescu, I., Schmides, J., & Lavallée, D. (2011). Effective friction law for small-scale fault heterogeneity in 3D dynamic rupture. *Journal of Geophysical Research*, 116(B10), B10306. <https://doi.org/10.1029/2010JB008118>
- Latour, S., Schubnel, A., Nielsen, S., Madariaga, R., & Vinciguerra, S. (2013). Characterization of nucleation during laboratory earthquakes. *Geophysical Research Letters*, 40(19), 5064–5069. <https://doi.org/10.1002/grl.50974>
- Lavallée, D. (2008). On the random nature of earthquake sources and ground motions: A unified theory. *Advances in Geophysics*, 50, 427–461. [https://doi.org/10.1016/S0065-2687\(08\)00016-2](https://doi.org/10.1016/S0065-2687(08)00016-2)
- Lebihain, M., Roch, T., Violay, M., & Molinari, J.-F. (2021). Earthquake nucleation along faults with heterogeneous weakening rate. *Geophysical Research Letters*, 48(21), e2021GL094901. <https://doi.org/10.1029/2021gl094901>
- McLaskey, G. C. (2019). Earthquake initiation from laboratory observations and implications for foreshocks. *Journal of Geophysical Research: Solid Earth*, 124(12), 12882–12904. <https://doi.org/10.1029/2019JB018363>
- Nadeau, R. M., & McEvilly, T. V. (1999). Fault slip rates at depth from recurrence intervals of repeating microearthquakes. *Science*, 285(5428), 718–721. <https://doi.org/10.1126/science.285.5428.718>
- Nielsen, S., Taddeucci, J., & Vinciguerra, S. (2010). Experimental observation of stick-slip instability fronts. *Geophysical Journal International*, 180(2), 697–702. <https://doi.org/10.1111/j.1365-246X.2009.04444.x>
- Ohnaka, M., & Shen, L.-F. (1999). Scaling of the shear rupture process from nucleation to dynamic propagation: Implications of geometric irregularity of the rupturing surfaces. *Journal of Geophysical Research*, 104(B1), 817–844. <https://doi.org/10.1029/1998jb900007>
- Passelègue, F. X., Latour, S., Schubnel, A., Nielsen, S., Bhat, H. S., & Madariaga, R. (2017). Influence of fault strength on precursory processes during laboratory earthquakes. *Fault Zone Dynamic Processes*, 229–242. <https://doi.org/10.1002/9781119156895.ch12>
- Rice, J. R., Lapusta, N., & Ranjith, K. (2001). Rate and state dependent friction and the stability of sliding between elastically deformable solids. *Journal of the Mechanics and Physics of Solids*, 49(9), 1865–1898. [https://doi.org/10.1016/S0022-5096\(01\)00042-4](https://doi.org/10.1016/S0022-5096(01)00042-4)
- Rubin, A. M., & Ampuero, J.-P. (2005). Earthquake nucleation on (aging) rate and state faults. *Journal of Geophysical Research*, 110(B11), B11312. <https://doi.org/10.1029/2005jb003686>
- Ruiz, S., Metois, M., Fuenzalida, A., Ruiz, J., Leyton, F., Grandin, R., et al. (2014). Intense foreshocks and a slow slip event preceded the 2014 Iquique M_w 8.1 earthquake. *Science*, 345(6201), 1165–1169. <https://doi.org/10.1126/science.1256074>
- Schär, S., Albertini, G., & Kammer, D. S. (2021). Nucleation of frictional sliding by coalescence of microslip. *International Journal of Solids and Structures*, 225, 111059. <https://doi.org/10.1016/j.ijsolstr.2021.111059>
- Schubnel, A., Nielsen, S., Taddeucci, J., Vinciguerra, S., & Rao, S. (2011). Photo-acoustic study of subshear and supershear ruptures in the laboratory. *Earth and Planetary Science Letters*, 308(3–4), 424–432. <https://doi.org/10.1016/j.epsl.2011.06.013>
- Sudhir, K., & Lapusta, N. (2020). Nucleation of earthquake slip on heterogeneous interfaces. In *Agü Fall Meeting Abstracts* (Vol. 2020, p. S026-05).
- Svetlizky, I., & Fineberg, J. (2014). Classical shear cracks drive the onset of dry frictional motion. *Nature*, 509(7499), 205–208. <https://doi.org/10.1038/nature13202>
- Uchida, N., Iinuma, T., Nadeau, R. M., Bürgmann, R., & Hino, R. (2016). Periodic slow slip triggers megathrust zone earthquakes in northeastern Japan. *Science*, 351(6272), 488–492. <https://doi.org/10.1126/science.1253108>
- Uchida, N., Matsuzawa, T., Hasegawa, A., & Igarashi, T. (2003). Interplate quasi-static slip off Sanriku, NE Japan, estimated from repeating earthquakes. *Geophysical Research Letters*, 30(15), 1801. <https://doi.org/10.1029/2003GL017452>
- Uenishi, K., & Rice, J. R. (2003). Universal nucleation length for slip-weakening rupture instability under nonuniform fault loading. *Journal of Geophysical Research*, 108(B1), 2042. <https://doi.org/10.1029/2001jb001681>
- Wu, B. S., & McLaskey, G. C. (2019). Contained laboratory earthquakes ranging from slow to fast. *Journal of Geophysical Research: Solid Earth*, 124(10), 10270–10291. <https://doi.org/10.1029/2019jb017865>
- Xia, K., Rosakis, A. J., & Kanamori, H. (2004). Laboratory earthquakes: The sub-Rayleigh-to-supershear rupture transition. *Science*, 303(5665), 1859–1861. <https://doi.org/10.1126/science.1094022>
- Xu, S., Fukuyama, E., Yamashita, F., Mizoguchi, K., Takizawa, S., & Kawakata, H. (2018). Strain rate effect on fault slip and rupture evolution: Insight from meter-scale rock friction experiments. *Tectonophysics*, 733, 209–231. <https://doi.org/10.1016/j.tecto.2017.11.039>
- Yabe, S., & Ide, S. (2018). Variations in precursory slip behavior resulting from frictional heterogeneity. *Progress in Earth and Planetary Science*, 5(1), 1–11. <https://doi.org/10.1186/s40645-018-0201-x>
- Yamashita, F., Fukuyama, E., Xu, S., Kawakata, H., Mizoguchi, K., & Takizawa, S. (2021). Two end-member earthquake preparations illuminated by foreshock activity on a meter-scale laboratory fault. *Nature Communications*, 12(1), 1–11. <https://doi.org/10.1038/s41467-021-24625-4>
- Yamashita, F., Fukuyama, E., Xu, S., Mizoguchi, K., Kawakata, H., & Takizawa, S. (2018). Rupture preparation process controlled by surface roughness on meter-scale laboratory fault. *Tectonophysics*, 733, 193–208. <https://doi.org/10.1016/j.tecto.2018.01.034>